PLASMA HEATING, PLASMA FLOW AND WAVE PRODUCTION AROUND AN ELECTRON BEAM INJECTED INTO THE IONOSPHERE

J. R. Winckler and K. N. Erickson
School of Physics and Astronomy, University of Minnesota
Minneapolis, Minnesota 55455

Abstract. A brief historical summary of the Minnesota ECHO series and other relevant electron beam experiments is given. The primary purpose of the ECHO experiments is the use of conjugate echoes as probes of the magnetosphere, but beam-plasma and wave studies have also been made. The measurement of quasi-DC electric fields and ion streaming during the ECHO 6 experiment has given a pattern for the plasma flow in the hot plasma region extending to 60m radius about the ECHO 6 electron beam. The sheath and potential well caused by ion orbits is discussed with the aid of a model which fits the observations. ELF wave production in the plasma sheath around the beam is briefly discussed. The new ECHO 7 mission to be launched from the Poker Flat range in November 1987 is described.

Introduction

This paper will be concerned mostly with results from the ECHO 6 electron beam sounding rocket experiment in which studies were made of the hot plasma regions, plasma flow and ELF wave production in the vicinity of the injected electron beam. The ECHO 6 mission is the latest in a coordinated series of electron beam experiments carried by large sounding rockets at ionospheric heights. The primary purpose of the experiments, beginning with the first launch in August 1970 from the NASA Wallops Island range in Virginia, has been to inject powerful pulses of electrons which travel in the outer magnetosphere, reflect from the magnetic conjugate region and return near the point of origin where under proper conditions they may be detected and analyzed. The original science objective, which was successfully carried out during the ECHO 1, 3, and 4 experiments has been to use these electron echoes as probes of the distant magnetosphere to study the dynamic morphology of the magnetic field in the nighttime sector by measuring bounce times and field line lengths, thus determining the degree of "inflation" of the magnetosphere during substorms and during the action of the tail current systems. Another objective has been to study the pitch angle diffusion and acceleration of the electrons to increase the understanding of the injection and acceleration of natural particles. Electron beams as probes are discussed by Winckler (1982). The geometry in space from the Poker Flat range in Alaska is shown schematically in Figure 1.

Electron beam experiments, a type of "active" experiment in the magnetosphere, have been carried out by a number of investigators. The Franco-Soviet ARAKS experiment (Cambou et.al., 1980), the Davis Kauai experiment (Davis et.al., 1980) and the ECHO series have been concerned with conjugate phenomena. Most other such experiments have had as their objective the study of the beam-plasma interaction in the ionosphere either for comparison with laboratory measurements of the beam plasma discharge or for studies of vehicle potentials and plasma wave production caused by the beam interaction. The ECHO series remains unique among electron beam experiments in retaining as the primary objective the study of conjugate echoes as outlined above. Following the original Hess Artificial Aurora experiment (Hess et.al., 1971), the ECHO series has emphasized optical and photometry measurements including low light level TV measurements of the artificial auroral streaks in the ionosphere, the luminosity around beam-emitting payloads, and the search for unstable luminosities around the beams (the beam plasma discharge) for which no adequate optical evidence has been obtained in space. The ECHO series has been successful also in studies of ELF frequency range wave spectra including ion resonances produced by the electron beam injections because of the high quality orthogonal electric field experiments carried by the ECHO 6
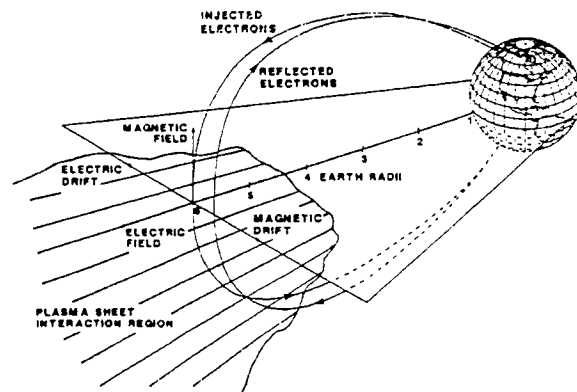

Figure 1. Magnetic field line geometry for nominal magnetic conditions from Alaska for conjugate echo trajectories.

mission. It is notable that electron beams can excite strong ion resonances and that this is a unique result from the sounding rocket type experiment and will probably not be accessible to orbiting plasma laboratories because of the high orbital speed through the plasma medium. An analysis of the ECHO 6 ELF waves and their possible sources is contained in the Ph.D. thesis of Yasuyuki Abe (Minnesota, 1986) and also in Winckler et.al. (1985). Electron beam experiments through 1979 have been reviewed by Winckler (1980).

Electron beam experiments have now been conducted on a number of flights of the Space Shuttle. A major experiment called SEPAC was carried on Spacelab-1 STS 9 and evolved essentially in the format suggested by the AMPS Study Group (Obayashi et.al., 1984). Other Shuttle-based electron beam experiments are reported by Shawhan et.al. (1983). These experiments will be discussed in detail elsewhere in this symposium. Orbiting plasma laboratories have in certain respects a high potential but are at the same time limited by their high speed through the ionospheric plasma and other factors in their ability to investigate natural phenomena in the magnetosphere.

ECHO 6 Plasma Studies

Experiment Details

We will be concerned with measurements of the perturbed plasma region in a cylindrical volume around an electron beam injected upwards from a rocket in the magnetosphere at 200 km altitude. The ECHO 6 mission included a Plasma Diagnostics Package (PDP) which was separated from the accelerator or main payload while the two sections were rotating about an axis inclined 20 degrees towards magnetic north from the local field vector. The PDP thus moved away from the main payload spinning at 0.5 rps as shown in Figure 2. The separation speed of 1.5 m/sec along the line of the PDP axis produced a slow increase in the radial distance of the PDP from the field line containing the beam. The accelerators were activated when the perpendicular radial distance was about 34m and continued to more than 100m. The accelerators were programmed in many modes, but we shall be concerned here mostly with beam injections at a pitch angle of 100 degrees, i.e. 10 degrees upwards from perpendicular, and also with injections at 180 degrees upwards parallel to B and downwards at 15 degree pitch angle. Data will be analyzed only in 50ms or 100ms intervals when only Gun 1 was operating, which produced discrete energy pulses from 20 KeV to a maximum of 36 KeV at 240 mA. The accelerator system is described elsewhere (Winckler et.al., 1984b). Two types of measurements will be analyzed;

firstly, those obtained with the PDP orthogonal electric field probes shown in Figure 2. The two pairs were sampled in differential, and also individually, with respect to the payload body each 0.4 msec, which permitted us to construct the instantaneous electric vector in a plane perpendicular to the magnetic field with 0.4 msec resolution and a Nyquist frequency of 1250 Hz; secondly, measurements were also made of the thermal ion spectra with the PDP electrostatic spectrometers which rotated with the PDP but viewed several different inclinations including the direction perpendicular to the PDP spin axis. The experiment included many other features which are described in several publications (Winckler et.al., 1984a; Winckler et.al., 1984b; Winckler et.al., 1985; Winckler et.al., 1986).

Hot Plasma

The heating of a plasma by an electron beam is a well recognized phenomenon and has been much discussed (see for example Grandal, Ed., 1982). The beam plasma interaction results in the electron beam kinetic energy being converted
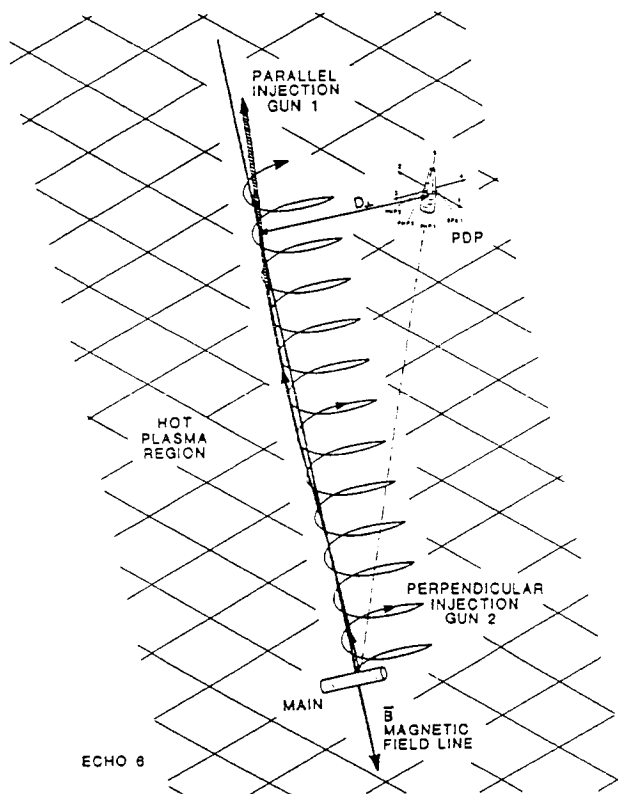
Figure 2. Geometry of the Plasma Diagnostics Package shown moving away from the main payload along its spin axis inclined 20 degrees to the magnetic field.

through basically the two-stream instability into turbulent electric fields similar to an RF discharge. These fields may be capable of accelerating the electrons in the ambient plasma to produce a discharge. This "beam plasma discharge" has been studied extensively in laboratory vacuum tanks and probably occurrs in space if the neutral density is sufficiently high (Galeev et.al., 1976; Hallinan et.al., 1984). Laboratory experiments, as well as the theoretical treatments of this subject, deal with the region close to the beam or even the region within the Larmor spiral of the beam itself. However, the ECHO 6 measurements clearly show that a much larger plasma region is heated and perturbed out to distances of 60m for the ECHO 6 beam which corresponds to 6 gyro radii from the beam center. This plasma region is heated very quickly, within 1 msec of beam turn-on, by a mechanism which must be an extension of the central beam plasma interaction but which certainly is not well understood. This hot plasma region contains strong electric fields generated by the beam as we shall discuss here in detail and also produces plasma and electromagnetic waves from the low ion gyro frequencies near 20 Hz up to very high frequencies probably up to the upper hybrid frequencies. Unfortunately, direct measurements of the plasma electron spectra or of the plasma parameters during beam injection were not obtained on the ECHO 6 experiment due to the failure of its electron spectrometer system and because the Langmuir probe was blocked by large floating potential changes of the PDP payload. Nevertheless, these floating potential changes, in themselves, provide a valuable measure of the hot plasma environment. They were observed by the probe-payload single potential differences and also could be observed by the shift in the low or cutoff energy of the ionospheric thermal ion spectra measured by the ion spectrometer. These two methods gave essentially the same result, but the minimum energy of the ions is a very convincing measure of the negative floating potential of the PDP with respect to plasma potential because the ions are accelerated through this potential difference from the ambient medium in order to reach the spectrometer. The use of this method has been developed by Arnoldy at the University of New Hampshire (Arnoldy and Winckler 1981) and others. That paper also presents good spectra of the hot electron plasma near the ECHO 3 beam-emitting rocket payload which may well be typical of the present ECHO 6 situation as well (see also Figure 7 in this paper). Electron and ion heating and acceleration by electron beams are discussed also in Arnoldy et.al. (1985) and by Winckler et.al. (1986). We show in Figure 3, in the lower panel; the PDP floating potentials as a function of flight time (bottom of figure) or perpendicular distance (top of figure) derived from the low

energy cutoff of the thermal ion spectra, and in the upper panels, the magnetic north and east components of the quasi-DC electric field measured by the PDP probes. The curves correspond to a "down" injection at 15 degrees, as well as the 100 degree "out" and 180 degree "up" directions. The largest effects are produced by "out" injections in which the beam spirals with a gyro radius of 10m and produces electric field and floating potential effects out to 50m. It is difficult to assign an electron temperature to the plasma on the basis of the floating potential measurements, but spectra previously obtained have characteristic temperatures of several eV and a continuously falling spectra reaching
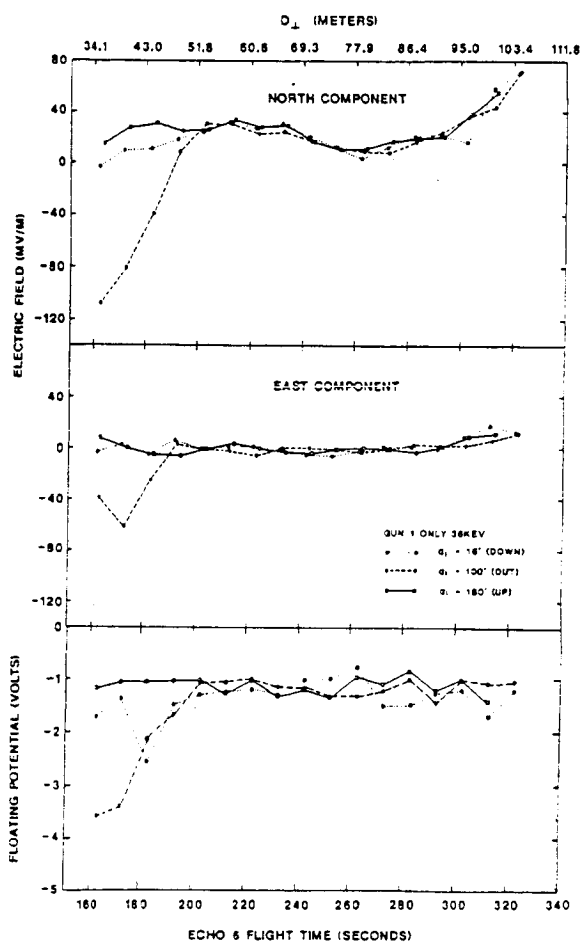

Figure 3. Electric field components in the earth reference frame showing the correlation of strong beam sector directed electric fields with the hot plasma region (lower panel floating potential). Perpendicular distance of the PDP from beam shown at top of figure.

297

nearly to the beam energy which in this case was 36 KeV.

Electric Fields

The quasi-DC electric field values shown in Figure 3 are averages over 50 msec intervals and represent the effects of the beam and the magnetospheric convection background in the earth reference frame but with wave frequencies higher than about 20Hz averaged out. These wave fields may be quite dramatic as shown by the example in Figure 4. This figure includes the effects of both accelerators and shows a strong low frequency rotating electric vector at 50 Hz (O+) and higher frequency components. The quasi-DC average field vector which has been subtracted is also shown and is typical of data used in constructing Figure 3. The north and east components of these average fields are negative, which means that the electric vector perpendicular to the magnetic field in the hot plasma region was directed inward but with a direction westward of the beam, while in the region outside the hot plasma beyond 50m, the fields showed only the predominately northward magnetospheric convection component. It is instructive to display these quasi-DC beam produced vector fields in the plane perpendicular to the magnetic field each 10s as the PDP moved away from the beam. To simplify the interpretation of the observed fields, the remaining vector field and flow patterns will be shown in the payload reference frame where the payload and the injected beam are at rest, and the observed field E' is given by E'= E + VXB where E is the total field in the earth reference frame and V is the rocket velocity perpendicular to B. Three such vector average E-field surveys are shown in Figure 5

corresponding to gun 1 only injecting down, out and up at 36 keV and 240 mA. The down injection passes by the PDP only after reflecting and scattering from the atmosphere 100 km below and produces little effect. The up injection is field aligned and passes the PDP which saw almost no effect in the range of radial distances surveyed beyond 40m. The large effects are produced by out injections spiralling almost perpendicular to the magnetic field. We note that as the flight progresses northward and descends, V decreases. When the PDP emerges from the hot plasma region near 60m (Figure 5, panel B) the strong inward fields disappear and the field vector E' rotates to an average northwesterly direction in the payload frame. This ionospheric field dominates the surveys in Figure 5 between 60m and the end of the data at 120m but in itself contains certain fluctuations characteristic of the ionosphere in the presence of an auroral arc. The ECHO 6 system did interact with an aurora, and we have discussed this in a previous publication (Winckler et.al., 1985).

At the beginning of data at accelerator turn-on, the PDP was about 34m radial distance from the beam and was 117m above the accelerator payload. It appears that very little effect was discerned of the positive potential of the main payload as shown by the lack of beam effect in Figure 5 panels A and C. but that the electric field patterns are those associated with the presence of the negative electron beam and the hot plasma surrounding it. Generally, the accelerator payload would be expected to have a potential of several hundred volts positive associated with the injection of the beam and the balance of the return currents from the ionospheric plasma. No direct payload potential
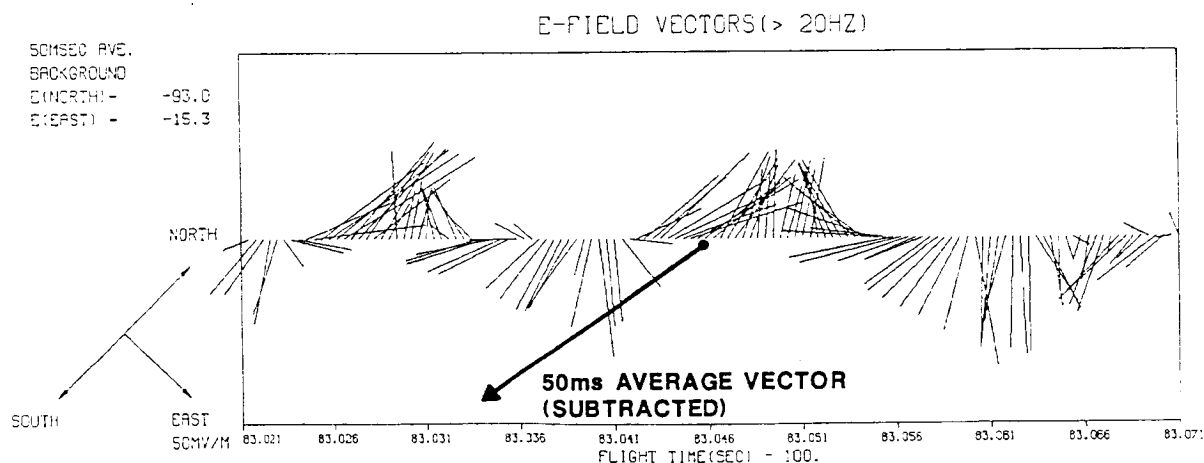

Figure 4. Maximum resolution data showing an electric field vector each 0.4 ms with the 50 ms average vector shown on the figure substracted. Earth reference frame. The rotational mode wave is probably an O+ gyro resonance.

measurements were made during the ECHO 6 experiment. Rocket payload potentials in the ionosphere have now been studied using deployable tethered subpayloads which give values in the range of several hundred volts and constitute the most reliable method to measure this potential (Raitt et.al., 1986). Figure 6 has been constructed to show not only the electric fields and flow directions corresponding to the gun 1 out injection but also a suggested hot plasma region, the beam geometry and reference dimensions. The unique plasma field with the ionospheric field in the rocket reference system subtracted is also shown as a dotted arrow. It is seen that none of the strong fields associated with the hot plasma are directed towards the beam. The question is "Why is this so?" and "What is the exact significance of these fields?" We must consider that the electron beam carries a negative space charge of significant proportions. This will be discussed somewhat later, but if the plasma fields were due to this space charge alone, one would expect symmetry around the beam gyro axis. There is also the problem that the PDP scan line in the magnetic perpendicular plane surveys only one radial region around the beam. Also, the measurements begin only at 34m radius which was the location of the PDP when the accelerator was turned on for

the first time.

Plasma Flow

With a little imagination it is possible to construct a potential field and flow lines along the equipotentials which correspond to the hydro-dynamical case of a single vortex located in a uniform stream. Such a diagram is shown in Figure 7. The field has been constructed by assuming an axisymmetrical potential around the beam and a uniform flow corresponding to E+VxB. Since the external flow field is known, it is possible to construct the flow lines based on an average over the region exterior to the hot plasma when only the ionospheric effects were present. The flow pattern is brought around the beam in such a way as to correspond to the electric vectors measured inside 60m radius, and then the interior is merely a series of circles. The exact negative potential of the circulating beam is not known. However, in the diagram shown, one can construct a potential well, and this has been done along the line X-X and is shown in Figure 8. For the case shown, the potential dips to about -5 volts as given by the "observed" line. The classic vacuum potential of a line charge, which more or less fits the right side of this potential, is given by the dotted

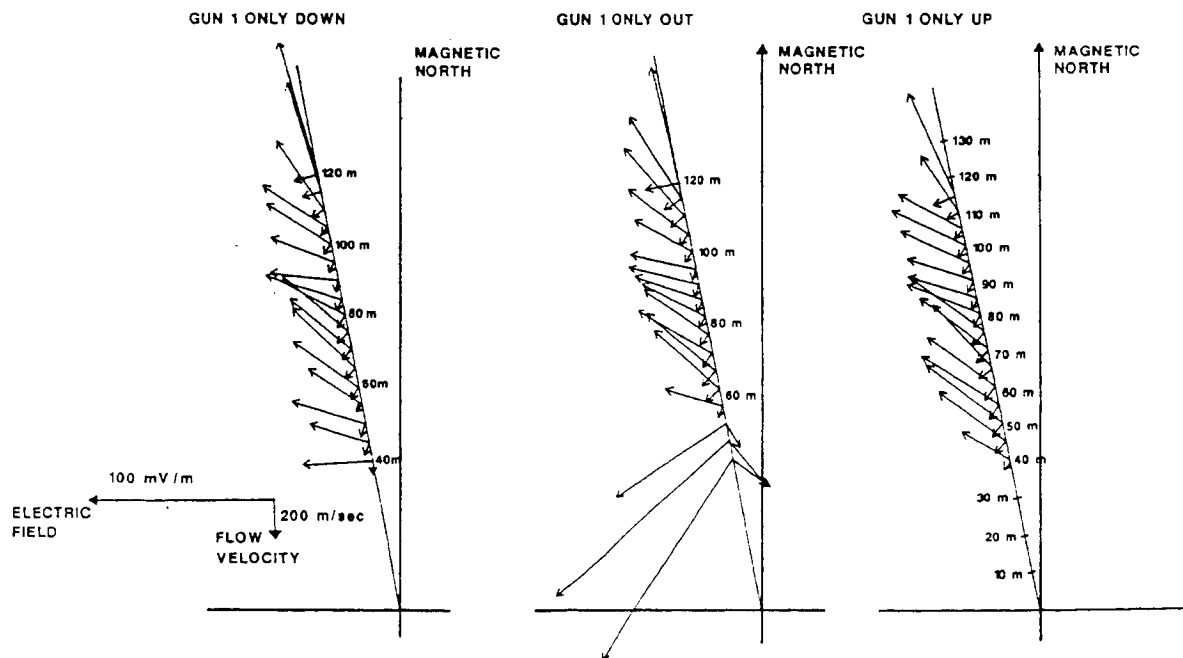**ELECTRIC FIELD AND FLOW VECTORS IN PAYLOAD REFERENCE FRAME**

Figure 5. The electric fileds and flow vectors in a plane perpendicular to B in the payload references frame. These are 50 ms averages for times when only Gun 1 was injecting at 36 KeV and 240 mA in the down, out, and up pitch angle configuration.

curve, and the constants are included. Of course, the radial potential profile is not simply that of a line charge even close to the beam because of the plasma sheath which forms around it. Also, the pattern is asymetrical due to the external flow influence. Nevertheless, the basic origins of the flow pattern shown in Figure 7 cannot be very different from that discussed here.

We have checked the flow by a completely independent method; namely, to observe the streaming or ram direction of ionospheric thermal ions with the ion spectrometer. Some scan data are shown in Figure 9. These have been ordered in ten-second blocks corresponding to the program for the two accelerators shown at the bottom. Of
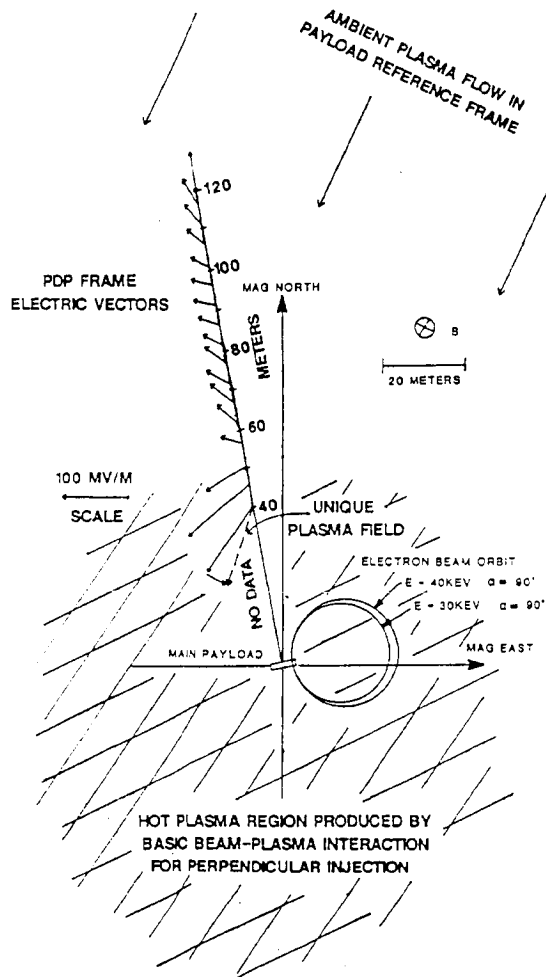
Figure 6. Summary of electric field and flow vectors in the payload references frame showing the beam and hot plasma region dimensions. Note the dotted arrow showing the unique plasma field with the ionospheric field subtracted.
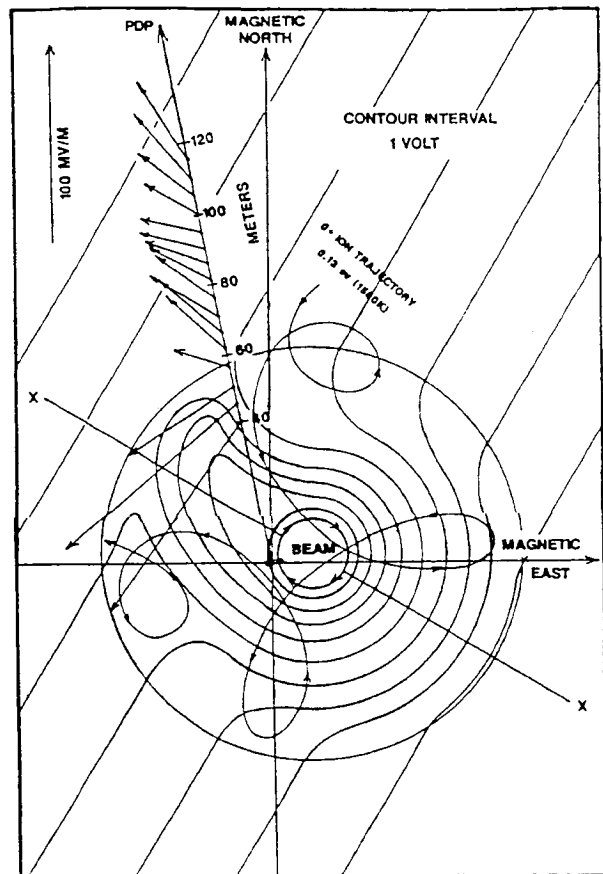
Figure 7. Flow patterns fitted to the observed electric fields for the out gun configuration. The circle shows the boundary of the hot plasma and beam associated electric field region. Contours within this region are very qualitative. A typical thermal ion trajectory is also shown. For the potential distribution along the line XX, see Figure 8.
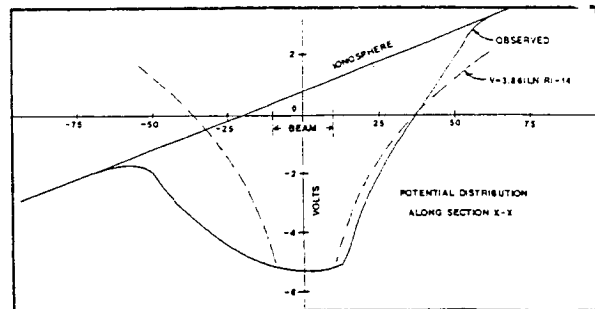
Figure 8. Transverse potential distribution along section XX in Figure 7. The electric field of a negative line charge in vacuum at the beam location is shown by the dashed curve.

particular interest is the down, the out and up configuration of Gun 1. The out configuration shown by the black bar corresponds to observing the thermal ions from a completely different direction than that characteristic of the background ionosphere traced out by the two outside parallel lines. At the top of the figure, the direction of observation is shown by a diagram. The center line corresponds to a direction nearly 150 degrees counterclockwise than normal. After the 170 second scan, the out configuration of the gun no longer coincides with the time at which the ion spectrometer could observe the ram direction of the thermal ions, and so a peak is not observed but only the systematic peaks on either side due to the "normal" ionosphere. However, even up to the 190 or 200 second traces, one can observe structure due to diversion of ions out of the normal pattern leaving gaps or irregularities caused by the turning on of the accelerator in blocks of time shown along the bottom line. We find that the ion measurements are in complete accord with the electric field boom measurements as regards the large shift in flow direction in the outer

part of the hot plasma region. One must note that due to the superposed beam-produced wave activity, the ions are further perturbed with short time structures which are extremely complex and which have not been analyzed in detail up to this time.

The Beam as a Cylindrical Charge

The generation of a sheath around the beam comes from the action of the coulombic negative potential of the beam plus the space charge produced by the orbiting ions and the presence of the plasma electrons. It has been possible to uncover a dependence of these plasma fields on the linear charge density of the beam, because during a portion of the gun program, the beam was stepped through a series of pitch angles around 90 degrees, thus altering the parallel velocity of the beam from downward to upward and slowly changing the pitch of the spiral and the linear charge density associated with it. In Figure 10, we show that effect in a series of scans over pitch angle at each of a number of radial
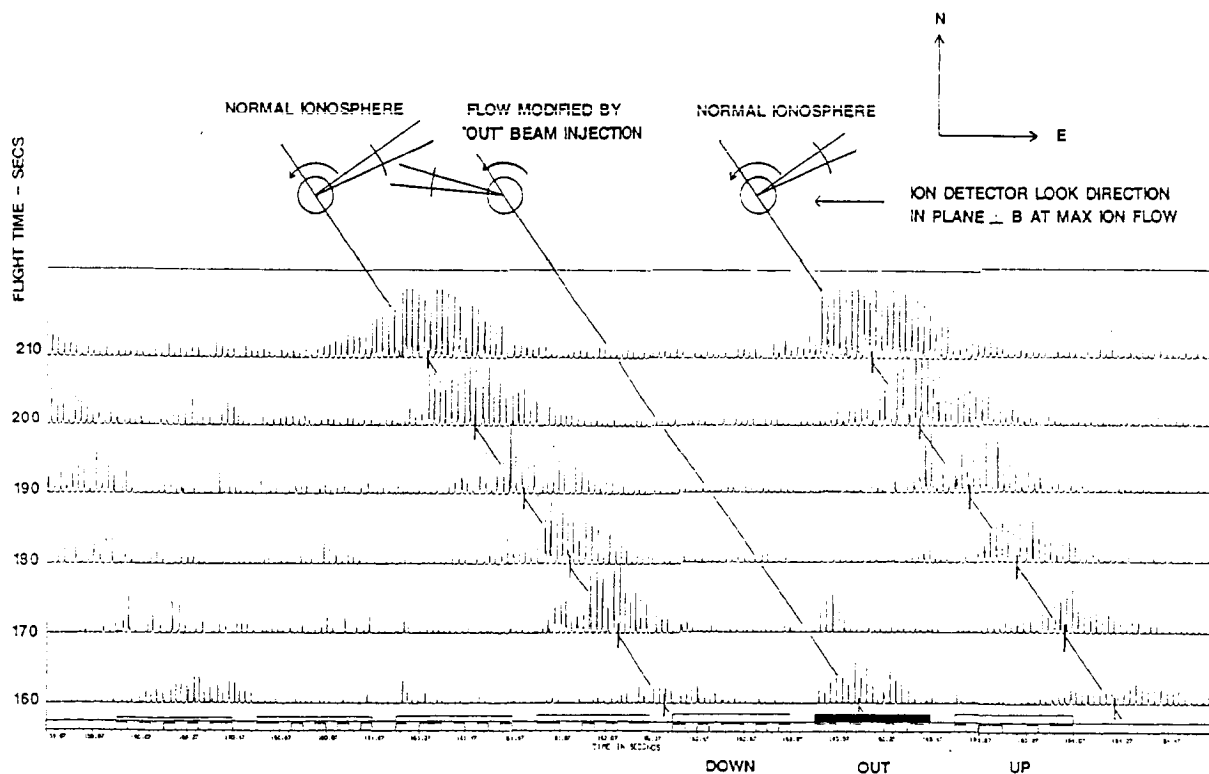

Figure 9. Ion drift detector (IDD) responses as the PDP rotated with a 2 second period. The data is organized by accelerator program times, so the times at which the ionospheric ion "ram" was seen lie on the indicated slant lines (ion look directions at top). During several accelerator "out" pulses, the ion "ram" direction is found approximately 140 degrees from the background flow direction, showing the effect of the accelerator-produced electric fields.

301

distances labelled on the curves in meters. It can be seen that downward injections at 88 degrees gave the smallest fields and that most of the curves maximize in the upward range between 90 degrees and 94 degrees, with a peak at 92 degrees. This is exactly what one would expect if we consider the divergence angle of the beam of about 2 degrees with the result that at 92 degrees all of the beam moves upward. The drop of the measured fields as the pitch angle increases can be caused by the decrease in linear density as the parallel velocity of the beam increases. Figure 10 was constructed when Gun 1 was injecting alone at a 15 KeV energy and a current of about 57 mA. The electric fields obtained with the full power of 36 KeV, 240 mA and a pitch angle of 100 degrees (called "out" injections) are actually similar to the peak values shown in Figure 10.

The equivalent cylindrical (or line) charge of the beam is given by $L(C/m) = I/((1.88 \times 10 \ast 7) K \ast 1/2 \cos a)$ where I is the beam current in amperes, K the energy in keV and a the pitch angle in degrees. Application of Gauss's law gives the electric field at distance R(m) as $E(mV/m) = 1.8 \times 10 \ast 13 \ L/R$ in a vacuum. Thus one obtains 9900 mV/m at 40m distance from a 15 keV 57mA beam at 92 degrees pitch angle in vacuum. This is about 100 times the observed range of values, a difference attributable to the neutralization of the beam charge by ions forming a sheath in the hot plasma region around the beam.

It is thus quite certain that we are observing the negative coulombic charge of the beam with its accompanying circulating flow imbedded in the
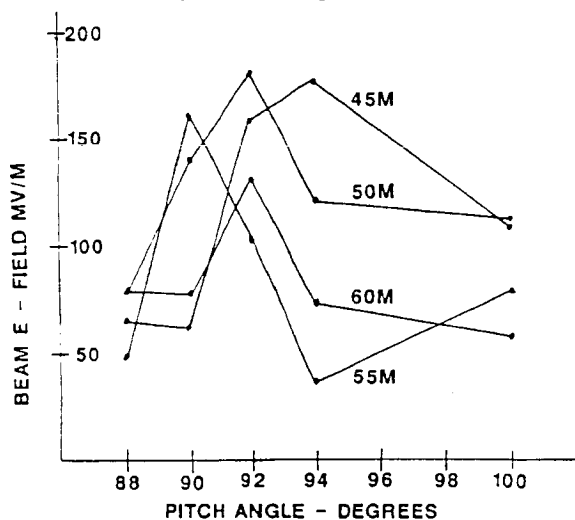

Figure 10. Average electric field in the payload reference system at various distances along the PDP survey line as a function of beam pitch angle near the perpendicular direction. Gun 1 only at 15 KeV, 57 mA.
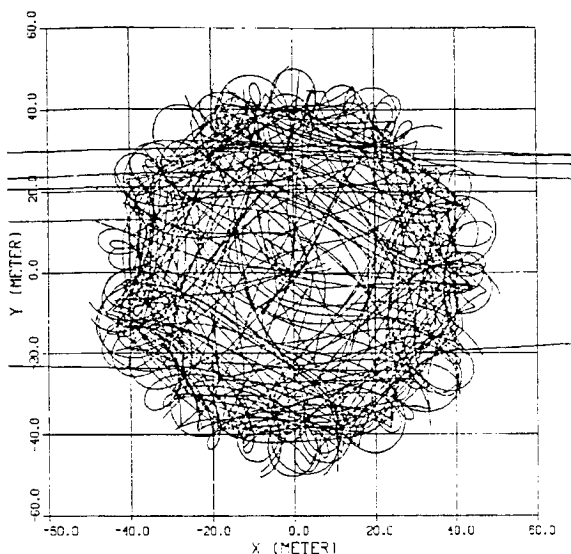
TRAJECTORY

Figure 11. Some typical thermal ion trajectories in a negative axisymmetric potential well. Courtesy of Y. Abe.

external uniform flow field of the ionosphere. It is in this framework that the various wave phenomena observed can arise. To derive theoretically a more exact potential for comparison with observations, one would have to do a self-consistent computation of the ion orbits in the classical vacuum potential of the beam and iterate the charge density in the sheath a number of times to converge on a final steady state solution for the sheath potential. We show in Figure 11, a figure constructed by Y. Abe to illustrate the first step in such a calculation. We have also shown in Figure 7 more or less to scale an orbit of an oxygen ion of 0.13 eV (1500 k) energy. This ion is drifting and precessing in the direction of the external flow lines, falls through the potential of the beam, accelerates and gyrates a few times before escaping. This trajectory is only for illustration and is not exact except in the external region.

ELF Wave Production

Finally, we comment on the ELF wave effects actually observed in the flow pattern shown here. The wave production depends strongly on the conditions of the observed beam injection such as the pitch angle, the type of beam with the discrete or the continuous energy spread from either Gun 1 or Gun 2 and also on the radial distance. The matrix-montage shown in Figure 12 was obtained from three configurations of Gun 1
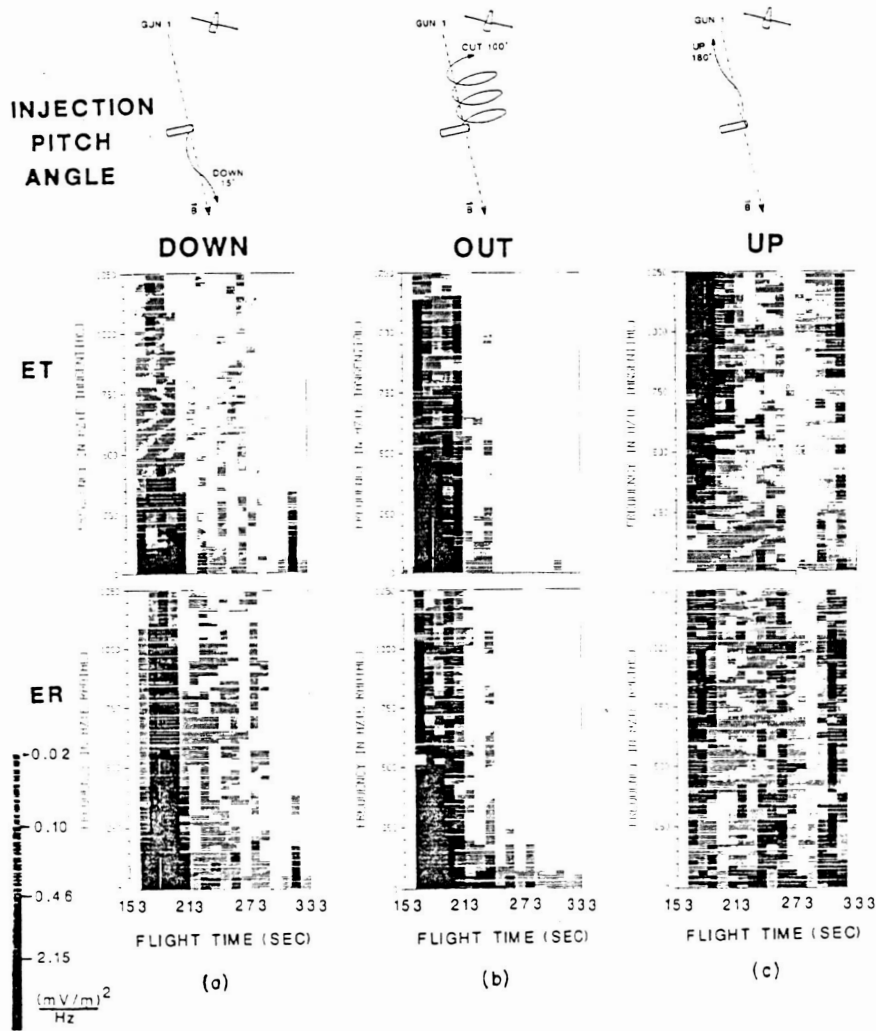
Figure 12. ELF wave spectrograms sorted according to down, out and up injections of Gun 1 only in the transverse and radial polarization components. Note that the up injection concentrates the wave energy towards the lower hybrid range above the 1250 Hz Nyquist frequency, but out and down injections are concentrated below 500 Hz. Intense wave activity is mainly in the hot plasma region (see lower panels). Wave activity dropped near 80 m when the system passed through auroral field lines.

at full power of 36 KeV and 240 mA when injected down, out or up and the wave spectrograms have been constructed for the transverse polarization and the radial polarization as a function of distance from the beam. We comment here only on the very striking fact that the downward and outward orientations produce large power at very low frequencies up to a radial distance corresponding closely to the hot plasma region. The upward injections, on the other hand, produce power largely in the transverse mode and reaching a maximum beyond our Nyquist frequency of 1250 Hz with low power below 200 Hz. It is in this configuration that a strong proton-gyro resonance has been observed as discussed in a previous publication (Winckler et.al., 1984). It has been suggested by Professor Paul Kellogg that low frequency waves generated in the hot plasma region may be due to a Buneman type instability caused by the rotating electron plasma passing through the randomized ion sheath (see also, Kellogg et.al., 1982).

The New ECHO 7 Mission

We are implementing a new ECHO mission which may be the last in the series and will be launched in November 1987 from the Poker Flat range in Alaska. This mission combines all of the experiences with the previous six flights to optimize both the conjugate echo and magnetospheric studies and the beam plasma physics. To guarantee the interception of echoes, ECHO 7 will be launched on a magnetically eastward trajectory like ECHOS 1, 2, 3, and 4. This will result in the interception of echoes during a limited portion of the flight. However, there will be four separate sections of the payload which are deployed, and all will be capable of echo detection. Two of these, a PDP like that used in the ECHO 6 mission described above and a second similar section called the Energetic Particle Package (EPP), will carry more sophisticated echo detectors in the form of large aperture electrostatic analyzers using microchannel plate detectors and amplifier systems. These energy spectrometers will be backed up by scintillation counters on all of the payloads and directed over a range of pitch angles. Since three of the subpayloads will be separated from the accelerator payload, the blanking of echo signals by the presence of the injected beam on the accelerator payload, as was encountered with the earlier ECHO flights, will be avoided. Also, the payloads will spread out in a certain region around the beam injecting field line as shown in Figure 13, which will increase the echo detection time during the flight. It is planned to launch the Terrier-Black Brandt (Black Brandt 9) eastward just to the south of a stable, discrete auroral arc in the presence of northerly magnetospheric convection electric fields in the evening sector of the magnetosphere. The experiment will thus be conducted in the diffuse auroral

region, and it will probably not be possible to cross the aurora as was accomplished with ECHO 6.

The mission includes extensive beam plasma studies. The nose cone will be equipped by the Kellogg group at Minnesota with a plasma waves analysis system and includes a Langmuir probe and a scintillation counter to detect beam energy particles. The nose cone experiment will be launched upward parallel to the magnetic field and will thus remain near the injected beam (reference Figure 13). The PDP will be injected to the south at a 10 degree angle to the magnetic field and will contain orthogonal electric booms, as in ECHO 6, for studying the ELF range up to 2500 Hz. It will also contain ion and electron spectrometers and an imaging ion spectrometer for searching for perpendicular ion acceleration near the beam. This payload will contain a television camera which will view the beam injecting payload continuously during the flight to study the
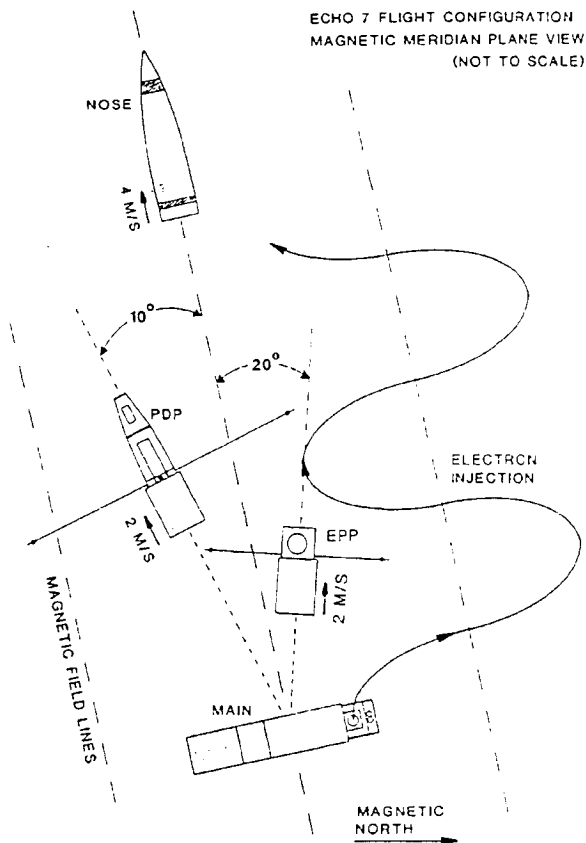

Figure 13. The ECHO 7 payload disposition in flight. Three deployable payload sections will carry wave and particle instrumentation, search for conjugate echoes and study plasma and electromagnetic radiation from the main accelerator payload.

distribution of luminosity in the hot plasma region. It will also contain arrays of photometers and the major echo detecting system described above. The EPP will contain a major plasma and electromagnetic wave detection system furnished by the Ernstmeyer group at the Air Force Geophysics Laboratory and will also include an orthogonal boom system in the ELF electric field range up to 1250 Hz. Both EPP and PDP will also carry magnetic antennas for wave studies. The main payload will contain a single accelerator of the type flown on ECHO 6, capable of 40 KeV maximum at 250 mA. This payload will be implemented in its entirety by the Malcolm group at the Air Force Geophysics Laboratory. It will have a magnetically controlled pitch angle system, and the payload will contain some photometric and particle detectors. This payload will also deploy a small tethered subflyer which will extend to several hundred meters distance and study the beam-emitting payload potentials with respect to the undisturbed plasma medium. The experiment is aimed at a comprehensive probing of the distant magnetosphere and also to extend the studies of the electric fields and plasma flow discussed in this paper with two-point measurements simultaneously in the flow pattern. It is also hoped to explore the origin of the hot plasma region and to investigate basic mechanisms of wave production by the electron beam over a very wide frequency range essentially from DC to above the upper hybrid frequency.

Acknowledgements

Bibliography

Abe, Y., Studies of a turbulent plasma environment near an electron-beam-emitting rocket in the polar ionosphere using electric probes: ECHO 6, Ph.D. Thesis, University of Minnesota, May 1986.

Arnoldy, R. L., and J. R. Winckler, The hot plasma environment and floating potentials of an electron-beam-emitting rocket in the ionosphere, J. Geophys. Res., 86, 575, 1981.

Arnoldy, R. L. and C. Pollock, The energization of electrons and ions by electron beams injected in the ionosphere, J. Geophys. Res., 90 5197, 1985.

Cambou, F., V. S. Dokoukine, J. Lavergnat, R. Pellat, H. Reme, A. Saint-Marc, R. Z. Sagdeev, and I. A. Zhulin, General description of the ARAKS experiments, Annales de Geophysique, 36, 271, 1980.

Davis, T. N., W. N. Hess, M. C. Trickel, E. M. Wescott, T. J. Hallinan, H. C. Stenbaek-Nielsen, and E. J. R. Maier, Artificial aurora conjugate to a rocket-borne electron accelerator, J. Geophys. Res., 85, 1722, 1980.

Galeev, A. A., E. V. Mishin, R. Z. Sagdeev, V. D. Shapiro, and V. I. Shevchenko, Discharge in the region around a rocket following injection of electron beams into the ionosphere (in Russian), Dokl. Akad. Nauk SSSR, 231, 71, 1976.

Grandal, B., editor, NATO Advanced Study Institute Series; Series B Physics, ed. Grandal, Plenum, New York, 79, 1982.

Hallinan, T. J., H. Leinback, G. Mantjoukis, and W. Bernstein, Measurements of the optical emission produced during the laboratory beam plasma discharge, J. Geophys. Res., 89, 2335, 1984.

Hess, W. N., M. G. Trichel, T. N. Davis, W. C. Beggs, G. E. Kraft, E. Stassinopoulos, and E. J. R. Maier, Artificial auroral experiment: Experiment and principal results, J. Geophys. Res., 76, 6067, 1971.

Kellogg, P. J., H. R. Anderson, W. Bernstein, T. J. Hallinan, R. H. Holzworth, R. J. Jost, H. Leinback, and E. P. Szuszczewicz, Laboratory simulation of injection particle beams, NATO Advanced Study Institue Series; Series B Physics, ed. Grandal, Plenum, New York, 79, 289, 1982.

Malcolm, P. R., Electron ECHO 6--a study by particle detectors of electrons artificially injected into the magnetosphere, Ph.D. Thesis, 1986.

Obayashi, T., et. al., Space experiments with particle accelerators, Science, 225, 195, 1984.

Raitt, W. J., N. B. Meyers, P. M. Banks, R. I. Bush, P. R. Williamson, N. Kawashima, K.-I. Oyama, S. Sasaki, and W. F. Sharp, CHARGE-2: An active vehicle charging rocket payload experiment, Symposium 1--Active Experiments, XXVI COSPAR 86, Toulouse, France.

Shawhan, S. D., J. L. Burch, and R. W. Fredericks, Subsatellite studies of wave, plasma and chemical injections from Spacelab, J. Spacecraft & Rockets, 20, 238, 1983.

Swanson, R. L., Electron ECHO 5--detection of artificially injected electrons by optical and x-ray methods, Ph.D. Thesis, University of Minnesota, June 1983.

Swanson, R. L., J. E. Steffen, and J. R. Winckler, The effect of strong pitch angle scattering on the use of artificial auroral streaks for echo detection--ECHO 5, Planet. Space Sci., 34, No. 5, 411, 1986.

Winckler, J. R., The application of artificial electron beams to magnetospheric research, Rev. Geophys. & Space Phys., 18, 659, 1980.

Winckler, J. R., The use of artificial electron beams as probes of the distant magnetosphere, NATO Advanced Study Institute Series; Series B Physics, ed. Grandal, Plenum, New York, 79, 3, 1982.

Winckler, J. R., J. E. Steffen, P. R. Malcolm, K. N. Erickson, Y. Abe, and R. L. Swanson, Ion resonances and ELF wave production by an electron beam injected into the ionosphere: ECHO 6, J. Geophys. Res., 89, 7565, 1984a.

Winckler, J. R., J. E. Steffen, P. R. Malcolm, K. N. Erickson, Y. Abe, and R. L. Swanson, Objectives and design of the ECHO 6 electron beam experiment; large ionospheric perturbations and energetic particle patterns, *Results of the ARCAD 3 Project and of the Recent Programmes in Magnetospheric and Ionospheric Physics*, ed. Centre National d'Etudes Spatiales, Toulouse, 713, 1984b.

Winckler, J. R., K. N. Erickson, Y. Abe, J. E. Steffen, and P. R. Malcolm, Elf wave production by an electron-beam-emitting rocket system and its suppression on auroral field lines: Evidence for Alfven and drift waves, *Geophys. Res. Lett.*, *12*, No. 7, 457, 1985.

Winckler, J. R., Y. Abe, and K. N. Erickson, Elf waves and ion resonances produced by an electron-beam-emitting rocket in the ionosphere, "Ion Acceleration in the Magnetosphere and Ionosphere," *Geophysical Monograph 38*, ed. T. Chang, AGU, 191, 1986.